Accepted for presentation at ISCRE 16, September 10-13, 2000, Cracow, Poland and publication in Chem. Engng Sci.

Hydrodynamic modeling of dense gas-fluidised beds using the kinetic theory of granular flow: effect of coefficient of restitution on bed dynamics

M.J.V. Goldschmidt, J.A.M. Kuipers, W.P.M. van Swaaij

Department of Chemical Engineering, Twente University, P.O. Box 217, 7500 AE Enschede, The Netherlands

Abstract

A two-dimensional multi-fluid Eulerian CFD model with closure laws according to the kinetic theory of granular flow has been applied to study the influence of the coefficient of restitution on the hydrodynamics of dense gas-fluidised beds. It is demonstrated that hydrodynamics of dense gas-fluidised beds (i.e. gas bubbles behaviour) strongly depend on the amount of energy dissipated in particle-particle encounters. It is concluded that, in order to obtain realistic bed dynamics from fundamental hydrodynamic models, it is of prime importance to correctly take the effect of energy dissipation due to non-ideal particle-particle encounters into account.

Keywords: fluidisation, multi-fluid model, kinetic theory of granular flow

1. Introduction

In the last decade considerable progress has been made in the area of hydrodynamic modeling of gas-fluidised suspensions. Broadly speaking two different classes of models can be distinguished, Eulerian (continuum) models and Lagrangian (discrete particle) models.
Lagrangian models solve the Newtonian equations of motion for each individual particle, taking into account the effects of particle collisions and forces acting on the particle by the gas. Particle collisions are described by collision laws, that account for energy dissipation due to non-ideal particle interactions by means of the empirical coefficients of restitution and friction (hard sphere approach, Hoomans et al., 1996) or an empirical spring stiffness, a dissipation constant and a friction coefficient (soft sphere approach, Tsuji et al., 1993).
The role of these collision parameters has been reported by several workers with respect to bubble formation and segregation in dense fluidised beds (Hoomans et al., 1996, 1998a; Hoomans 2000) and cluster formation in risers (Hoomans et al., 1998b; Ouyang and Li, 1999).
Eulerian models consider all phases to be continuous and fully interpenetrating. The equations employed are a generalisation of the Navier-Stokes equations for interacting continua. Owing to the continuum representation of the particulate phases, Eulerian models require additional closure laws to describe the rheology of the fluidised particles. In most recent continuum models constitutive equations according to the kinetic theory of granular flow are incorporated. This theory is basically an extension of the classical kinetic theory to dense particle flow, which provides explicit closures that take energy dissipation due to non-ideal particle-particle collisions into account by means of the coefficient of restitution.
An extreme, unrealistic, sensitivity of Eulerian models due to inelastic particle-particle collisions has been reported by several authors for simulations of riser flow (Pita and Sundaresan, 1991; Nieuwland et al., 1996; Hrenya and Sinclair, 1997). In this study a two-dimensional multi-fluid Eulerian CFD model has been applied to study the influence of the coefficient of restitution on the hydrodynamics of dense gas-fluidised beds.

2. Multi-fluid model

In the multi-fluid Eulerian model the particle mixture is divided into a discrete number of classes, whereby different physical properties can be specified for each particle class. The governing equations for the multi-fluid model are given in table 1, whereby the granular temperature of phase k is defined as:

$$\theta_k = \frac{1}{3} < \overline{C}_k \cdot \overline{C}_k >$$

Several authors have worked on the derivation of constitutive equations for binary and multi-component mixtures based on the kinetic theory of granular flow (Jenkins and Mancini 1987, 1989; Gidaspow, 1994; Manger, 1996; Mathiesen, 1997). The constitutive equations shown in table 2 where taken from Mathiesen and adapted to be consistent with the kinetic theory closures derived by Nieuwland (Nieuwland et al., 1996).

Table 1. Multi-fluid model, governing equations

Continuity equations

$$\frac{\partial(\varepsilon_k \rho_k)}{\partial t} + \nabla \cdot (\varepsilon_k \rho_k \bar{u}_k) = 0$$

Momentum equations

$$\frac{\partial(\varepsilon_k \rho_k \bar{u}_k)}{\partial t} + \nabla \cdot (\varepsilon_k \rho_k \bar{u}_k \bar{u}_k) = -\varepsilon_k \nabla p - \nabla P_k - \nabla \cdot (\varepsilon_k \bar{\bar{\tau}}_k) + \sum_{l=0}^{NP} \beta_{kl} (\bar{u}_l - \bar{u}_k) + \sum_{l=0}^{NP} \bar{b}^c_{kl,cor} + \varepsilon_k \rho_k \bar{g}$$

Pseudo-thermal energy equations

$$\frac{3}{2}\left\{\frac{\partial}{\partial t}(\varepsilon_k \rho_k \theta_k) + \nabla \cdot (\varepsilon_k \rho_k \theta_k \bar{u}_k)\right\} = -\left(P_k \bar{\bar{I}} + \varepsilon_k \bar{\bar{\tau}}_k\right) : \nabla \bar{u}_k + \nabla \cdot \bar{q}_k - \gamma_k - 3\beta_{k0}\theta_k$$

3. Two-fluid simulations

To study the influence of the coefficient of restitution on the hydrodynamics of a mono-disperse powder in a dense gas-fluidised bed, a number of two-fluid simulations was performed. Results obtained for various values of the coefficient of restitution where compared to experimental results obtained in a pseudo two-dimensional setup. The experimental conditions and simulation settings are specified in table 3.

The collision properties of the particles used in the experiment were obtained from detailed impact measurements preformed by the Impact Research Group of the Open University at Milton Keynes, where an accurate technique to measure collision parameters has been developed (Kharaz et al., 1999). The collision parameters are given in table 4.

Table 4. Collision properties (Gorham and Kharaz, 1999)

Particle-particle collisions	*Particle-wall collisions*
e = 0.97 ± 0.01	e = 0.97 ± 0.01
μ = 0.15 ± 0.015	μ = 0.10 ± 0.01
β_0 = 0.33 ± 0.05	β_0 = 0.33 ± 0.05

To reduce numerical diffusion the second order accurate Barton scheme (Centrella and Wilson, 1984; Hawley et al., 1984) was applied to discretise the convective fluxes in the governing equations. Grid refinement was studied, but the grid size did not have a significant influence on the obtained results. For the gas phase no-slip boundary conditions where used, the partial slip conditions applied to the particle phase are given by (Sinclair and Jackson, 1989):

$$\left(\bar{\bar{I}} - \bar{n}\bar{n}\right) \cdot \varepsilon_k \bar{\bar{\tau}}_k \cdot \bar{n} = \frac{f_{wall} \pi \varepsilon_k \rho_k g_0 \sqrt{\theta_k}}{2\sqrt{3}\varepsilon_{kl,max}} \bar{u}_k$$

$$\varepsilon_k \bar{q}_k \cdot \bar{n} = -\bar{u}_k \cdot \varepsilon_k \bar{\bar{\tau}}_k \cdot \bar{n} + \frac{\sqrt{3}\pi\left(1 - e^2_{k,wall}\right)\varepsilon_k \rho_k g_0 \sqrt{\theta_k}}{4\varepsilon_{kl,max}} \theta_k$$

In all simulations the minimum fluidisation condition was used as initial condition, where after the gas inflow velocity was stepwise set to $1.5 \cdot u_{mf}$. Small perturbations were applied to the initial particle volume fraction and the gas inflow velocity at the bottom, to improve resemblance with experimental conditions and avoid unrealistic start up behaviour due to perfect symmetry of the numerical solution.

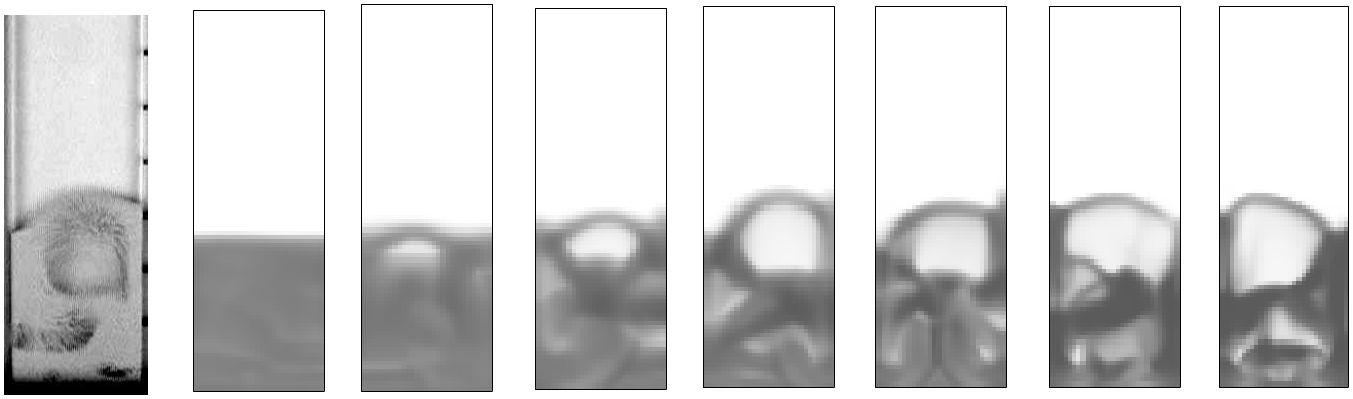

experiment e = 1.00 e = 0.99 e = 0.97 e = 0.95 e = 0.90 e = 0.80 e = 0.73

Fig. 1. Comparison between experiment and simulated bubbles for various values of the coefficient of restitution.

Table 2. Multi-fluid model, constitutive equations

Gas phase density

$$\rho_0 = \frac{M_0}{RT_0}\, p$$

Stresses

$$\bar{\bar{t}}_k = -\left\{\left(\lambda_k - \frac{2}{3}\mu_k \right)\left(\nabla \cdot \bar{u}_k\right)\bar{\bar{I}} + \mu_k\left(\left(\nabla \bar{u}_k\right) + \left(\nabla \bar{u}_k\right)^T \right)\right\}$$

Particle pressures

$$P_k = \sum_{l=1}^{NP} P_{kl}^c + \varepsilon_k\, \rho_k \theta = \sum_{l=1}^{NP} \frac{\pi}{3}(1+e_{kl}) d_{kl}^3 g_0 n_k n_l \left[\frac{m_k m_l m_{kl} \theta_k \theta_l}{(m_k^2\theta_k + m_l^2\theta_l)}\right]\left[\frac{m_{kl}^2 \theta_k \theta_l}{(m_k^2\theta_k + m_l^2\theta_l)(\theta_k + \theta_l)}\right]^{3/2} + \varepsilon_k\, \rho_k \theta_k$$

$$g_0 = 1 + 4(1-\varepsilon_0)\frac{1 + 2.5000\,(1-\varepsilon_0) + 4.5904\,(1-\varepsilon_0)^2 + 4.515439\,(1-\varepsilon_0)^3}{\left(1 - \left(\frac{1-\varepsilon_0}{\varepsilon_{kl,max}}\right)^3\right)^{0.67802}}$$

$$e_{kl} = \frac{1}{2}(e_k + e_l) \qquad d_{kl} = \frac{1}{2}(d_k + d_l) \qquad m_{kl} = (m_k + m_l)$$

Shear viscosities

$$\mu_k = \sum_{l=1}^{NP} \frac{P_{kl}^c}{\varepsilon_k}\frac{d_{kl}}{5}(m_k\theta_k + m_l\theta_l)\sqrt{\frac{2}{\pi\theta_k\theta_l(m_k^2\theta_k + m_l^2\theta_l)}} + 1.01600\,\frac{5}{16}\frac{m_k}{d_k^2}\sqrt{\frac{\theta_{k,av}}{\pi}}\,\frac{1}{\varepsilon_k g_0}\left(1 + \frac{4}{5}\sum_{l=1}^{NP} g_0 \varepsilon_l (1+e_{kl})\right)\left(1 + \frac{8}{5}\sum_{l=1}^{NP} g_0 \varepsilon_l\right)$$

$$\theta_{k,av} = \frac{2\theta_k}{\left[\sum_{l=1}^{NP}\left(\frac{n_l}{n_k}\right)\left(\frac{d_{kl}}{d_k}\right)^2\left(\frac{m_{kl}^2\theta_l}{(m_k^2\theta_k + m_l^2\theta_l)}\right)^{1/2}\left(\frac{m_{kl}^2\theta_k\theta_l}{(m_k^2\theta_k + m_l^2\theta_l)(\theta_k+\theta_l)}\right)^{3/2}\right]^2}$$

Bulk viscosities

$$\lambda_k = \sum_{l=1}^{NP} \frac{P_{kl}^c}{\varepsilon_k}\frac{d_{kl}}{3}(m_k\theta_k + m_l\theta_l)\sqrt{\frac{2}{\pi\theta_k\theta_l(m_k^2\theta_k + m_l^2\theta_l)}}$$

Pseudo-thermal energy fluxes

$$\bar{q}_k = \varepsilon_k \kappa_k \nabla\theta_k + \bar{q}_{k,cor}^c$$

$$q_{k,cor}^c = \sum_{l=1}^{NP} P_{kl}^c (1-e_{kl})\left\{\frac{9}{5}\frac{m_l}{m_{kl}}(\bar{u}_l - \bar{u}_k) + d_{kl}\left[\sqrt{\frac{2m_l^2\theta_l}{\pi(m_k^2\theta_k + m_l^2\theta_l)}}\left(\nabla ln\frac{\varepsilon_k}{\varepsilon_l} + 3\nabla\frac{ln(m_l\theta_l)}{ln(m_k\theta_k)}\right) + \right.\right.$$

$$\left.\left. 3\sqrt{\frac{2m_k^3\theta_k m_l^3\theta_l}{\pi(m_k^2\theta_k + m_l^2\theta_l)}}\left(\frac{m_l\theta_k\theta_l}{\theta_k+\theta_l}\left(\frac{\nabla\theta_k}{\theta_k^2} - \frac{\nabla\theta_l}{\theta_l^2}\right) + 6m_l\left(\frac{2m_k^3 m_l^3\theta_k\theta_l}{m_k^2\theta_k + m_l^2\theta_l}\right)^{3/2}\left(\frac{\nabla\theta_k}{m_k\theta_k^2} - \frac{\nabla\theta_l}{m_l\theta_l^2}\right)\right)\right]\right\}$$

Table 2. Continued

Pseudo-thermal conductivities

$$\kappa_k = 2\rho_k d_k \sqrt{\frac{\theta_k}{\pi}} \sum_{l=1}^{NP} \varepsilon_l g_0 (1+e_{kl}) + 1.02513 \frac{75}{64} \frac{m_k}{d_k^2} \sqrt{\frac{\theta_{k,av}}{\pi}} \frac{1}{\varepsilon_k g_0} \left(1+\frac{6}{5}\sum_{l=1}^{NP} \varepsilon_l g_0 (1+e_{kl})\right)\left(1+\frac{12}{5}\sum_{l=1}^{NP} \varepsilon_l g_0\right)$$

Pseudo-thermal energy dissipation

$$\gamma_k = \sum_{l=1}^{NP} \frac{3}{4} P_{kl}^c \frac{(1-e_{kl})}{d_{kl}} \left[4\sqrt{\frac{2m_{kl}^2 \theta_k \theta_l}{\pi (m_k^2 \theta_k + m_l^2 \theta_l)}} - d_{kl} \left(\frac{m_{kl} m_k \theta_k + m_{kl} m_l \theta_l}{m_k^2 \theta_k + m_l^2 \theta_l} \right) \nabla \cdot \bar{u}_k \right]$$

Interphase momentum transfer

gas-particle drag

$$\beta_{k0} = \beta_{0k} = \begin{cases} 150 \dfrac{(1-\varepsilon_0)\varepsilon_k}{\varepsilon_0} \dfrac{\mu_0}{(\phi_k d_k)^2} + 1.75 \varepsilon_k \dfrac{\rho_0}{(\phi_k d_k)} \left|\bar{u}_0 - \bar{u}_k\right| & \varepsilon_0 \le 0.8 \\ \dfrac{3}{4} C_{d,k} \dfrac{\varepsilon_0 \varepsilon_k}{(\phi_k d_k)} \rho_0 \left|\bar{u}_0 - \bar{u}_k\right| \varepsilon_0^{-2.65} & \varepsilon_0 > 0.8 \end{cases}$$

$$C_{d,k} = \begin{cases} \dfrac{24}{\mathrm{Re}_k}\left(1+0.15(\mathrm{Re}_k)^{0.687}\right) & \mathrm{Re}_k < 1000 \\ 0.44 & \mathrm{Re}_k \ge 1000 \end{cases}$$

$$\mathrm{Re}_k = \frac{\varepsilon_0 \rho_0 \left|\bar{u}_0 - \bar{u}_k\right| d_k}{\mu_0}$$

$$\bar{\beta}_{k0,cor}^c = \bar{\beta}_{0k,cor}^c = 0$$

particle-particle drag

$$\beta_{kl} = P_{kl}^c \frac{3}{d_{kl}} \sqrt{\frac{2(m_k^2 \theta_k + m_l^2 \theta_l)}{\pi m_{kl}^2 \theta_k \theta_l}}$$

$$\bar{\beta}_{kl,cor}^c = P_{kl}^c \left[\nabla\left(\ln \frac{\varepsilon_k}{\varepsilon_l} \right) + \frac{\theta_k \theta_l}{\theta_k + \theta_l} \left(\frac{\nabla \theta_l}{\theta_l^2} - \frac{\nabla \theta_k}{\theta_k^2} \right) + 3\nabla\left(\frac{\ln(m_l \theta_l)}{\ln(m_k \theta_k)} \right) + \frac{5}{3} \frac{m_{kl} \theta_k \theta_l}{m_k^2 \theta_k + m_l^2 \theta_l} \left(\frac{\nabla \theta_l}{m_l \theta_l^2} - \frac{\nabla \theta_k}{m_k \theta_k^2} \right) \right]$$

Table 3. Experimental conditions and simulation settings for two-fluid simulations

Height of experimental setup	70.0	cm	Freeboard pressure, P_0	101325.0 Pa
Width of experimental setup	15.0	cm	Temperature, T_0	293 K
Depth of experimental setup	1.50	cm	Gas phase shear viscosity, μ_0	$1.8 \cdot 10^{-5}$ Pa·s
			Gas phase bulk viscosity, λ_0	0.0 Pa·s
Initial bed height, h_b	15.0	cm		
Fluidisation velocity, u_{grid}	1.38	m/s	Particle diameter, d_1	1.50 mm
			Particle density, ρ_1	2523 kg/m^3
Horizontal grid size, Δx	5.0	mm	Particle shape factor, ϕ_1	1
Vertical grid size, Δz	5.0	mm	Minimum fluidisation velocity, u_{mf}	0.92 m/s
Number of grid cells in horizontal direction, nx	30		Minimum fluidisation porosity, ε_{mf}	0.417
Number of grid cells in vertical direction, nz	90			

Figure 1 shows snapshots of the experiment and simulations for various values of the coefficient of restitution at the moment of bubble eruption at the bed surface. It can be seen that as collisions become less ideal (and more energy is dissipated due to inelastic collisions) particles become closer packed in the densest regions of the bed, resulting in sharper porosity contours and larger bubbles. In simulations with ideal particles bubble formation did not appear for fluidisation velocities below $3 \cdot u_{mf}$.

To gain more insight into the influence of the coefficient of restitution on bed dynamics, a detailed study of all contributions to the pseudo-thermal energy equation was performed. Therefore the averages of all sources and sinks of fluctuating kinetic energy in the pseudo-thermal energy equation where calculated, e.g. for the contribution of particle pressure:

$$< P_k \bar{\bar{I}} : \nabla \bar{u}_k >= \frac{1}{18nxnz} \int_{t=2}^{20} \sum_{i=1}^{nx} \sum_{j=1}^{nz} \left(P_k \bar{\bar{I}} : \nabla \bar{u}_k \right)_{i,j} dt$$

For the calculation of these averages the initial 2 seconds of the simulations where not taken into account in order to avoid start-up effects from influencing the results (the total simulation time was 20 seconds). The average production of fluctuating kinetic energy due to particle pressure and viscous shear and dissipation due to inelastic collisions and gas-particle drag are shown in figure 2, the contribution due to conduction to the walls of the system was negligible. Also the weighted averages of the particle phase state variables, granular temperature and particle pressure, and the rheologic properties where computed, e.g. for the granular temperature:

$$< q_k >= \frac{1}{18 \sum_{i=1}^{nx} \sum_{j=1}^{nz} e_{k,i,j}} \int_{t=2}^{20} \sum_{i=1}^{nx} \sum_{j=1}^{nz} e_{k,i,j} q_{k,i,j} dt$$

The results are shown in figures 3 and 4.

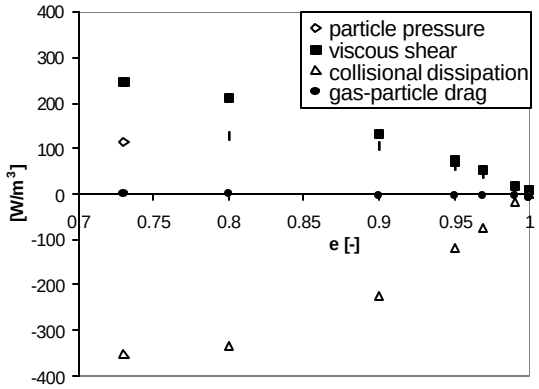

Fig. 2. Average contribution of sources and sinks in the pseudo-thermal energy equation as a function of the coefficient of restitution

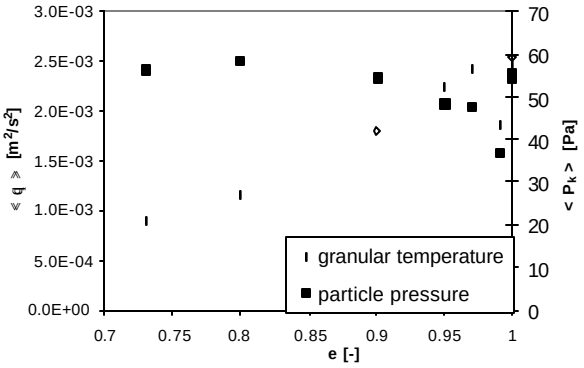

Fig. 3. Average particle phase state variables as a function of the coefficient of restitution

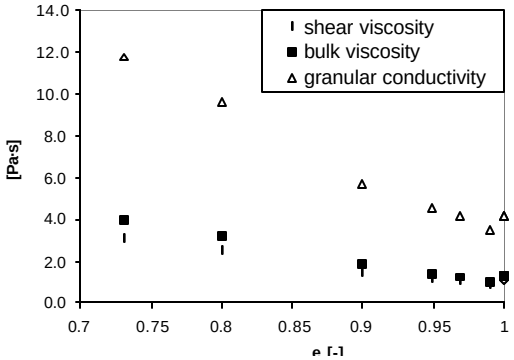

Fig. 4. Average viscosities and conductivity as a function of the coefficient of restitution.

From figure 2 it can be seen that as the coefficient of restitution decreases and particle interactions become less ideal, more fluctuating kinetic energy is generated by particle pressure and viscous shear. This energy is almost completely dissipated by inelastic deformation of particles upon collision, while dissipation by gas-particle drag hardly contributes.

Figure 3 shows that the granular temperature decreases as particle interactions become less ideal, even though figure 2 shows that the energy production rates increase. The particle pressure remains relatively constant.

From figure 4 it can be concluded that the fluidised particle mixture becomes more viscous if the coefficient of restitution decreases. Further the average shear viscosity is in good agreement with measured values of 0.1-2.6 Pa·s (Schügerl et al., 1961; Stewart, 1968; Grace, 1970).

To show the effect of the coefficient of restitution on bed dynamics the computed instantaneous pressure drop over the bed is presented in figure 5 for three cases with different values for the coefficient of restitution. It can be observed that pressure fluctuations depend strongly on the coefficient of restitution. When more energy is dissipated simulations show stronger pressure fluctuations (i.e. more vigorous bubbling).

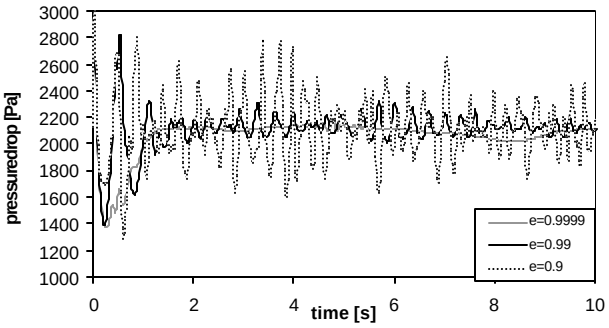

Fig. 5. Fluctuations of pressure drop over the bed for various values of the coefficient of restitution.

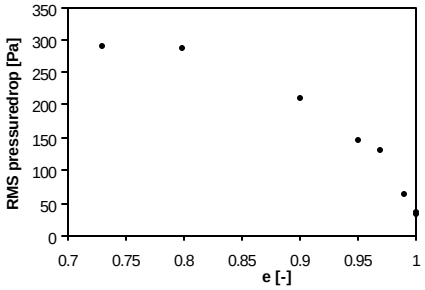

Fig. 6. Root Mean Square (RMS) of pressure drop fluctuations as a function of coefficient of restitution

In figure 6 the root mean square (RMS) of the pressure fluctuations is presented as a function of the coefficient of restitution (the initial 2 seconds of the simulations where again not taken into account). From the figure it can be seen that the intensity of pressure fluctuations in the bed decreases gradually when the coefficient of restitution approaches 1. Further the model does not show extreme sensitivity with respect to the coefficient of restitution. These results are consistent with those obtained from discrete particle simulations of dense beds (Hoomans et al., 1998a).

It can also be observed from figure 1 that the simulation with e=0.97 does not show the best resemblance with the experiment. This can be explained from the fact that the total energy dissipation during a collision results from inelastic deformation as well as from frictional slip (Johnson, 1985). Hence the total energy dissipation will also depend upon the friction coefficient and the coefficient of tangential restitution. Hoomans (Hoomans, 2000) applied a discrete particle model to study the effect of all three particle collision properties on the hydrodynamics of dense gas-fluidised beds. From this work it was concluded that pressure fluctuations in dense beds depend upon the total amount of energy dissipated by both inelastic and frictional contributions. Further it was concluded that the influence of the tangential coefficient of restitution was negligible for realistic values of the coefficient of friction.

A simple approach to obtain the correct amount of energy dissipation has been suggested by Jenkins (Jenkins, 1999). For small coefficients of friction ($\mu<0.15$) the coefficient of restitution could be corrected to account for energy dissipation due to frictional losses:

$$e_{eff} = e - \frac{p}{2}m.$$

This correction results in an effective coefficient of restitution of 0.73. However from snapshots and movies of the experiment and the simulations it could be observed that the simulated bubble dynamics is to vigorous for e_{eff} =0.73 and the best resemblance between the experiment and simulations is obtained for e_{eff}=0.9. Moreover it should be noted here that the kinetic theory of granular flows has been derived for slightly inelastic spheres and application of the theory for e<0.9 is doubtful.

A kinetic theory for rapid granular flow of dense, slightly inelastic, slightly rough spheres that takes energy dissipation due to frictional losses into account has been developed by Lun and co-workers (Lun and Savage, 1987; Lun, 1991). So far this theory has not been applied to fluidised suspensions. However this might be necessary to obtain the correct amount of energy dissipation and bed dynamics. Further research in this area is required.

4. Multi-fluid simulations

It is well known that gas bubbles play an important role in mixing and segregation of particle mixtures in dense gas-fluidised beds (Rowe et al. 1972; Kunii and Levenspiel, 1991). Apart from their influence on bubble dynamics as shown in the previous section, particle collision properties will also directly influence momentum transfer between particles of different classes. Therefore prediction of segregation rates and patterns is a rather severe test case for fundamental hydrodynamic models and consequently the influence of the coefficient of restitution on segregation of a binary particle mixture of glass beads was studied. The particle properties are given in table 5, further the same conditions as for the two-fluid simulations where applied.

Initially the particles are well mixed and fluidised at the minimum fluidisation velocity of the smallest particles. At t=0 the fluidisation velocity is set to 1.30 m/s, which slightly exceeds u_{mf} of the biggest particles. The obtained segregation patterns for two values of the coefficient of restitution are shown in figure 7.

Table 5. Particle properties for multi-fluid simulations

Small particles	*Big particles*
d_1 = 1.50 mm	d_2 = 2.50 mm
ρ_1 = 2523 kg/m^3	ρ_2 = 2526 kg/m^3
$u_{mf,1}$ = 0.92 m/s	$u_{mf,2}$ = 1.28 m/s

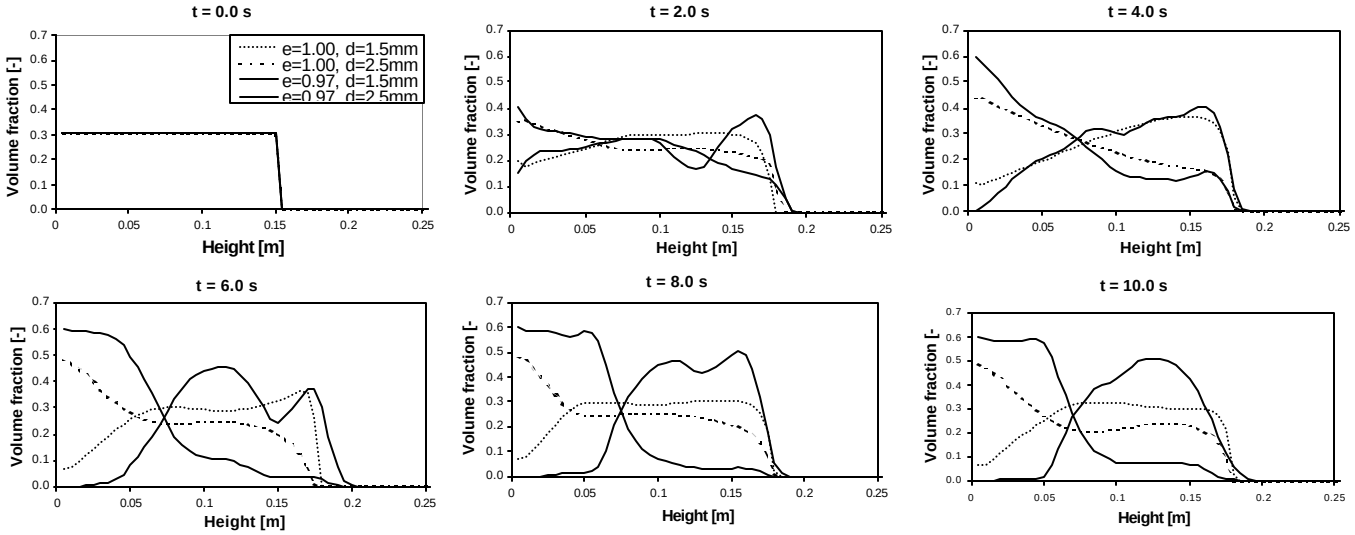

Fig. 7. Influence of coefficient of restitution on segregation of a binary particle mixture.

The figures show the spatially averaged volume fractions of both particle sizes as a function of the height in the bed. Within 10 seconds almost complete segregation is predicted when particle-particle interactions are non-ideal (e=0.97) and bubbles are present, while segregation is much slower when particle-particle interactions are ideal (e=1) and no bubbles are present. These results indicate that the segregation process is indeed directly influenced by particle-particle interactions..

Further it appears that segregation in the simulation with realistic collision parameters (e=0.97) occurs much quicker than in experiments, where complete segregation is obtained after only 60 seconds. Therefor special attention needs to be paid to the role of particle-particle interactions in dense gas-fluidised particle mixtures in future research. A digital image analysis technique to study segregation rates and patterns in a pseudo-two dimensional setup is currently under development and more attention will be paid to validation of the modeling results in the near future.

5. Conclusion

It is demonstrated that hydrodynamics of dense fluidised beds strongly depend on the amount of energy dissipated in particle-particle encounters. In order to obtain realistic simulations using fundamental hydrodynamic models it is of prime importance to correctly take the effect of non-ideal particle-particle encounters into account. Further development of the kinetic theory of granular flow seems necessary to improve the constitutive equations for multi-fluid continuum models. In this sense discrete particle models, which allow for a more detailed description of particle-particle and particle-wall interactions can be a useful tool. Since sensible validation of fundamental hydrodynamic models can only be made when collision parameters of the particles are set to the correct values, there is a great need for experiments with systems for which the particle collision parameters have been accurately determined.

Acknowledgement

The authors which to acknowledge the Unilever Research Laboratory for the financial support of this work, Dr. D.A. Gorham of the Impact Research Group of the Open University at Milton Keynes for the measurements of the collision parameters and Ir. R.C. Braam for his contribution to the implementation of the kinetic theory equations.

Nomenclature

C	= fluctuating component of particle velocity, m/s
C_d	= drag coefficient, kg/(m^{3}s)
d	= particle diameter, m
e	= coefficient of restitution
g	= gravity, m/s^2
g_0	= radial distribution function
M_0	= molar mass of gas, kg/mol
m	= particle mass, kg
n	= particle number density, m^{-3}
nx	= number of grid cells in horizontal direction
nz	= number of grid cells in vertical direction
p	= pressure, Pa
P	= particle pressure, Pa
q	= granular temperature flux, W/m^2
R	= gas constant, J/(mol·K)
Re	= Reynolds number
t	= time, s
T_0	= gas temperature, K
u	= velocity, m/s

β = drag, kg/(m^{3}s)
β_0 = tangential coefficient of restitution
Δx = size of grid cells in horizontal direction, m
Δz = size of grid cells in vertical direction, m
ε = volume fraction
$\varepsilon_{kl,max}$ = maximum particle fraction of particle mixture
ϕ = shape factor
ϕ_{wall} = specularity factor for particle-wall collisions
γ = dissipation due to inelastic collisions, W/m^3
κ = granular conductivity coefficient, Pa·s
λ = shear viscosity, Pa·s
μ = bulk viscosity, Pa·s
μ = friction coefficient
θ = granular temperature, m^2/s^2
ρ = density, kg/m^3
τ = stress tensor, Pa

References

Centrella, J., Wilson, J.R., 1984, Planar numerical cosmology. II**.** The difference equations and numerical tests, *Ap. J. Suppl*., **54**, 229-249

Gidaspow, D., 1994, *Multiphase flow and fluidisation*, Academic Press, London

Gorham, D.A., Kharaz, A.H., 1999, Results of particle impact tests, *Impact Research Group Report IRG 13*, The Open University, Milton Keynes, UK

Grace, J.R., 1970, The viscosity of fluidised beds, *Can. J. Chem. Engng*, **48**, 30-33

Hawley, J.F., Smarr, L.L., Wilson, J.R., 1984, A numerical study of nonspherical black hole accretion. II. Finite differencing and code calibration, *Ap. J. Suppl*., **55**, 211-246

Hoomans, B.P.B., Kuipers, J.A.M., Briels, W.J., Van Swaaij, W.P.M., 1996, Discrete particle simulation of bubble and slug formation in a two-dimensional gas-fluidised bed: a hard sphere approach, *Chem. Engng Sci*., **51**, 99-118

Hoomans, B.P.B., Kuipers, J.A.M., Van Swaaij, W.P.M., 1998a, The influence of particle properties on pressure signals in dense gas-fluidised beds: a computer simulation study, *World Congress on Particle Technology 3*, July 7-9, Brighton, UK

Hoomans, B.P.B., Kuipers, J.A.M., Van Swaaij, W.P.M., 1998b, Granular dynamics simulation of cluster formation in riser flow, *Third international conference on multiphase flow, ICMF'98*, June 8-12, Lyon, France

Hoomans, B.P.B., 2000, *Granular dynamics of gas-solid two-phase flows*, Ph.D. dissertation, Twente University, Enschede, The Netherlands

Hrenya, C.M., Sinclair, J.L., 1997, Effects of particle-phase turbulence in gas-solid flows, AIChE J., **43**, 853-869

Jenkins, J.T., Mancini, F., 1987, Balance laws and constitutive relations for plane flows of a dense, binary mixture of smooth, nearly elastic, circular disks, *J. Appl. Mech*., **54**, 27-34

Jenkins, J.T., Mancini, F., 1989, Kinetic theory for binary mixtures of smooth, nearly elastic spheres, *Phys. Fluids A 1*, **12**, 2050-2057

Jenkins, 1999, private communication

Johnson, 1985, *Contact mechanics*, Cambridge University Press, Cambrigde, UK

Kharaz, A.H., Gorham, D.A., Salman, A.D., 1999, Accurate measurement of particle impact parameters, *Measurement Science and Technology*, **10**, 31-35

Kunii, D., Levenspiel, O., 1991, *Fluidisation Engineering*, 2nd edition, Butterworth-Heinemann, Boston

Lun, C.K.K., Savage, S.B., 1987, A simple kinetic theory for granular flow of rough, inelastic, spherical particles, *J. Appl. Mech*., **54**, 47-53

Lun, C.K.K., 1991, Kinetic theory for granular flow of dense, slightly inelastic, slightly rough spheres, J. Fluid Mech., **233**, 539-559

Manger, E., 1996, *Modelling and simulation of gas/solids flow in curvelinear coordinates*, Telemark College, Department of Technology, Porsgrunn, Norway

Mathiesen, V., 1997, *An experimental and computational study of multiphase flow behaviour in circulating fluidised beds*, Telemark Institute of Technology, Porsgrunn, Norway

Nieuwland, J.J., Van Sint Annaland, M., Kuipers, J.A.M., Van Swaaij, W.P.M., 1996, Hydrodynamic modeling of gas/particle flows in riser reactors, *AIChE J.*, **42**, 1569-1582

Ouyang, J., Li, J., 1999, Discrete simulations of heterogeneous structure and dynamic behaviour in gas-solid fluidisation, *Chem. Engng. Sci*., **54**, 5427-5440

Pita, J.A., Sundaresan, S., 1991, Gas-solid flow in vertical tubes, *AIChE J*., **37**, 1009-1018

Rowe, P.N., Nienow, A.W., Agbim, A.J., 1972, The mechanism by which particles segregate in gas fluidised beds - binary systems of near-spherical particles, *Trans. Instn Chem. Engrs*, **50**, 310-323

Schügerl, K., Merz, M., Fetting, F., 1961, Rheologische Eigenschaften von gasdurchströmten Fleissbettsystemen, *Chem. Engng Sci*., 1961, **15**, 1-38

Sinclair, J.L., Jackson, R., 1989, Gas-particle flow in a vertical pipe with particle-particle interactions, *AIChE J*., **35**, 1473-1486

Stewart, P.S.B., 1968, Isolated bubbles in fluidised beds – theory and experiment, *Trans. Instn Chem. Engrs*, **46**, 60-66

Tsuji, Y., Kawaguchi, T., Tanaka, T., 1993, Discrete particle simulation of two-dimensional fluidised bed, Powder Technol., **77**, 79-87